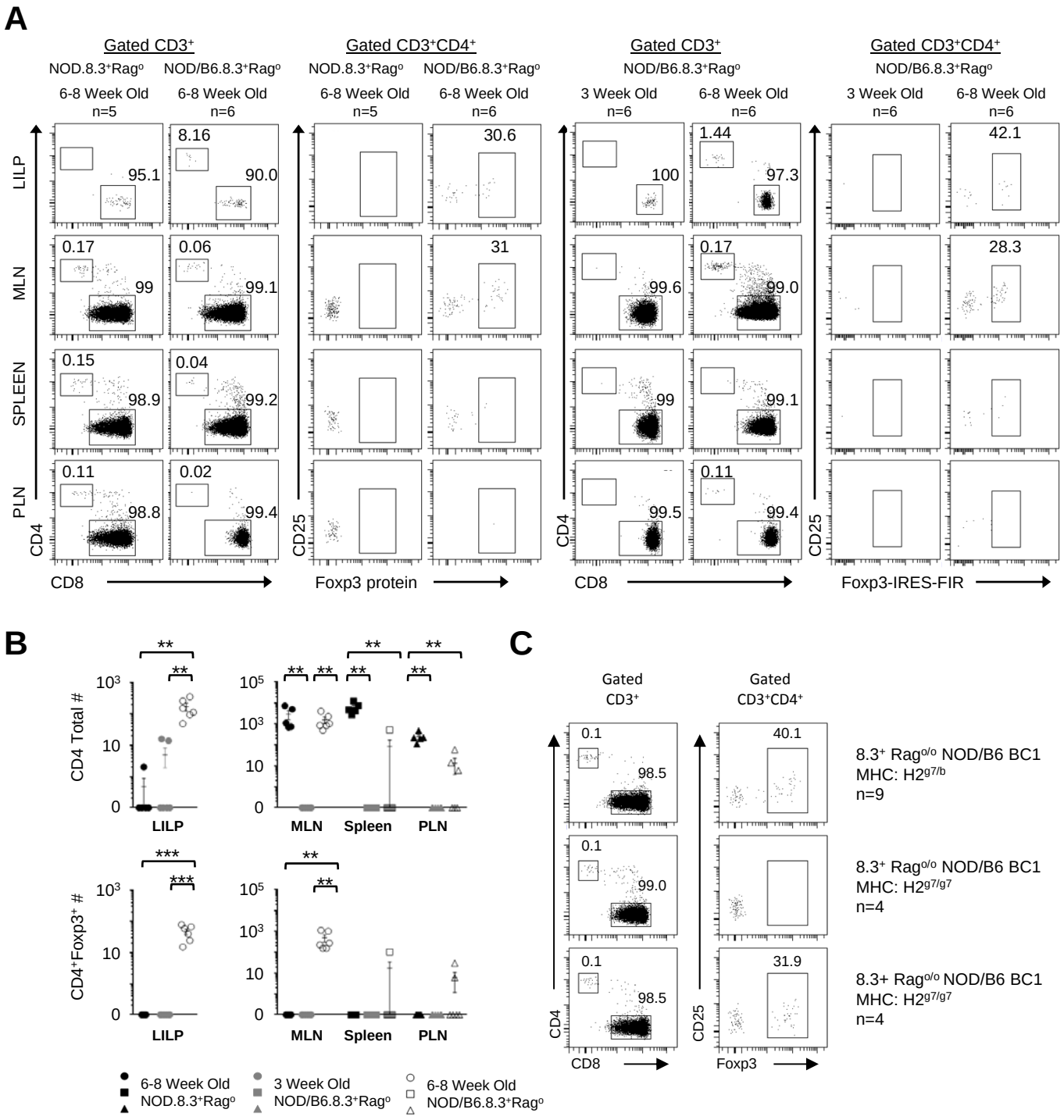
A
Gated CD3+
Gated CD3+CD4+
Gated CD3+
Gated CD3+CD4+
NOD.8.3+Rago
NOD/B6.8.3+Rago
6-8 Week Old
3 Week Old
n=5
n=6
LILP
MLN
SPLEEN
PLN
CD4
CD8
CD25
Foxp3 protein
Foxp3-IRES-FIR
B
CD4 Total #
CD4+Foxp3+ #
LILP
MLN
Spleen
PLN
6-8 Week Old NOD.8.3+Rago
3 Week Old NOD/B6.8.3+Rago
6-8 Week Old NOD/B6.8.3+Rago
C
Gated CD3+
Gated CD3+CD4+
Foxp3
8.3+ Rago/o NOD/B6 BC1
MHC: H2g7/b
n=9
8.3+ Rago/o NOD/B6 BC1
MHC: H2g7/g7
n=4
8.3+ Rago/o NOD/B6 BC1
MHC: H2g7/g7
n=4

Figure S1

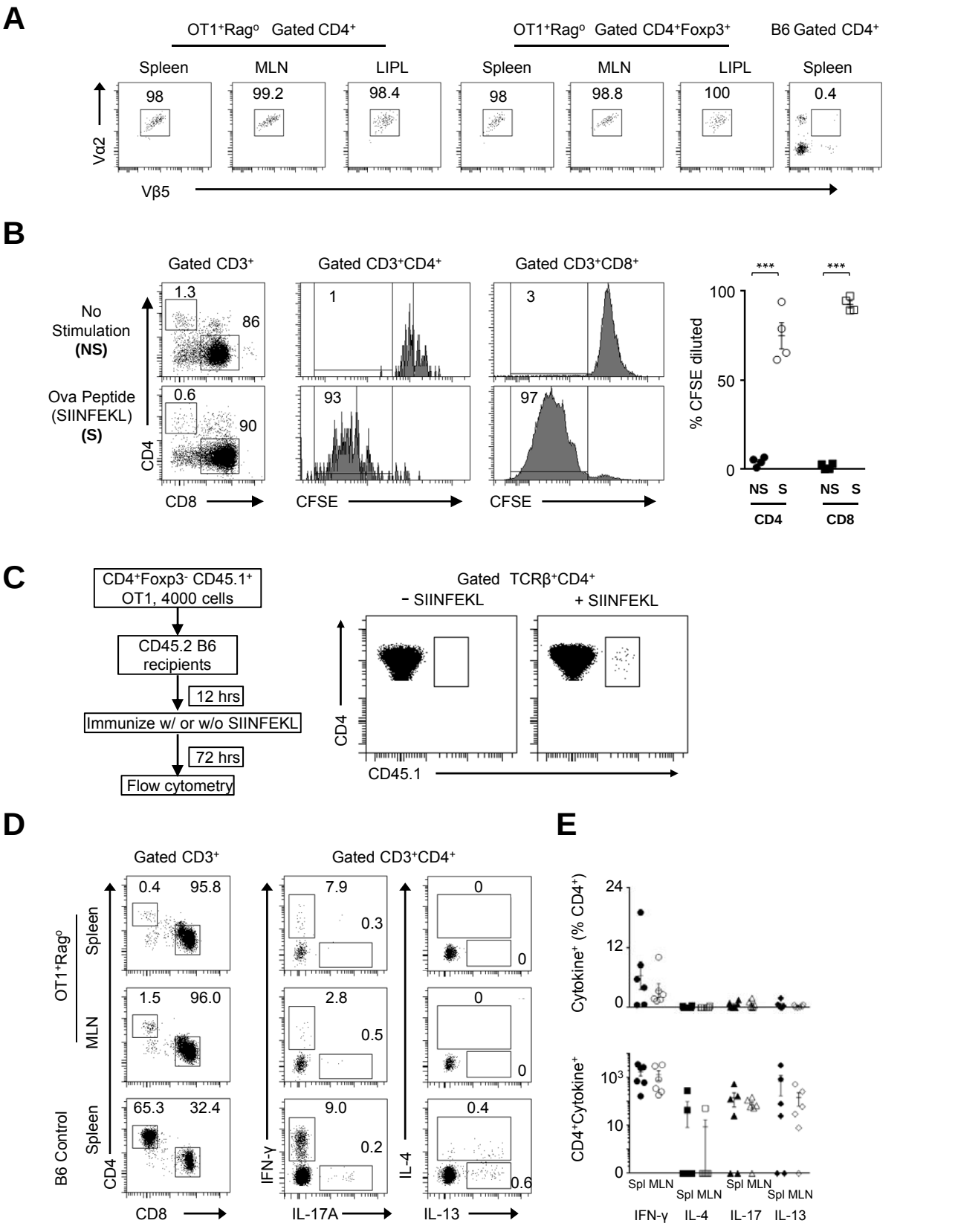
A
OT1+Rag° Gated CD4+
OT1+Rag° Gated CD4+Foxp3+
B6 Gated CD4+
Spleen
MLN
LIPL
Spleen
MLN
LIPL
Spleen
98
99.2
98.4
98
98.8
100
0.4
Vα2
Vβ5
B
Gated CD3+
Gated CD3+CD4+
Gated CD3+CD8+
No Stimulation (NS)
Ova Peptide (SIINFEKL) (S)
1.3
86
0.6
90
1
93
3
97
CD4
CD8
CFSE
CFSE
***
***
100
50
0
% CFSE diluted
NS S
NS S
CD4
CD8
C
CD4+Foxp3- CD45.1+ OT1, 4000 cells
CD45.2 B6 recipients
12 hrs
Immunize w/ or w/o SIINFEKL
72 hrs
Flow cytometry
Gated TCRβ+CD4+
- SIINFEKL
+ SIINFEKL
CD4
CD45.1
D
Gated CD3+
Gated CD3+CD4+
OT1+Rag°
Spleen
MLN
B6 Control
Spleen
0.4
95.8
1.5
96.0
65.3
32.4
7.9
0.3
2.8
0.5
9.0
0.2
0
0
0
0
0.4
0.6
CD4
CD8
IFN-γ
IL-17A
IL-4
IL-13
E
Cytokine+ (% CD4+)
24
12
0
CD4+Cytokine+
10^3
10
0
Spl MLN
Spl MLN
Spl MLN
Spl MLN
IFN-γ
IL-4
IL-17
IL-13

Figure S2

A

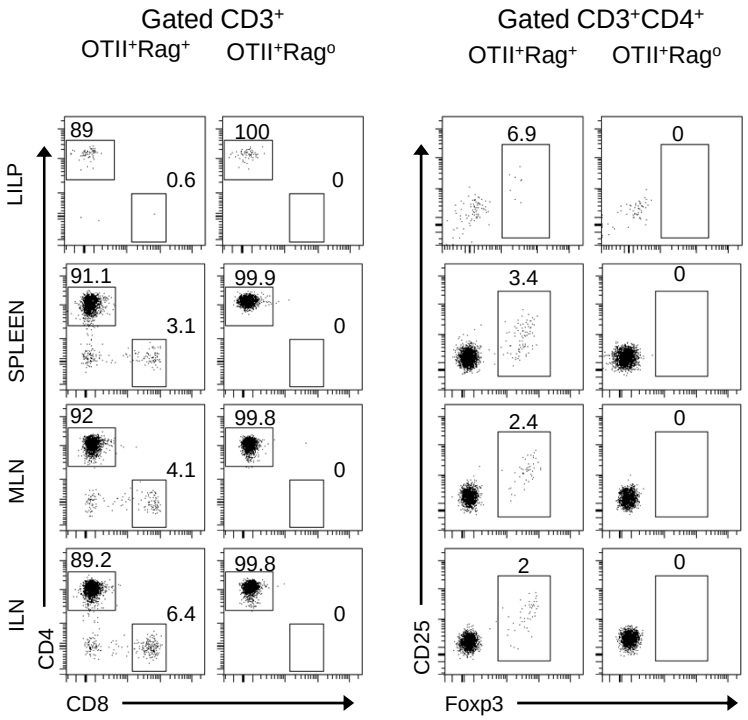
Gated CD3+
OTII+Rag+
OTII+Rago
Gated CD3+CD4+
OTII+Rag+
OTII+Rago
LILP
SPLEEN
MLN
ILN
89
0.6
100
0
91.1
3.1
99.9
0
92
4.1
99.8
0
89.2
6.4
99.8
0
6.9
0
3.4
0
2.4
0
2
0
CD4
CD8
CD25
Foxp3

B

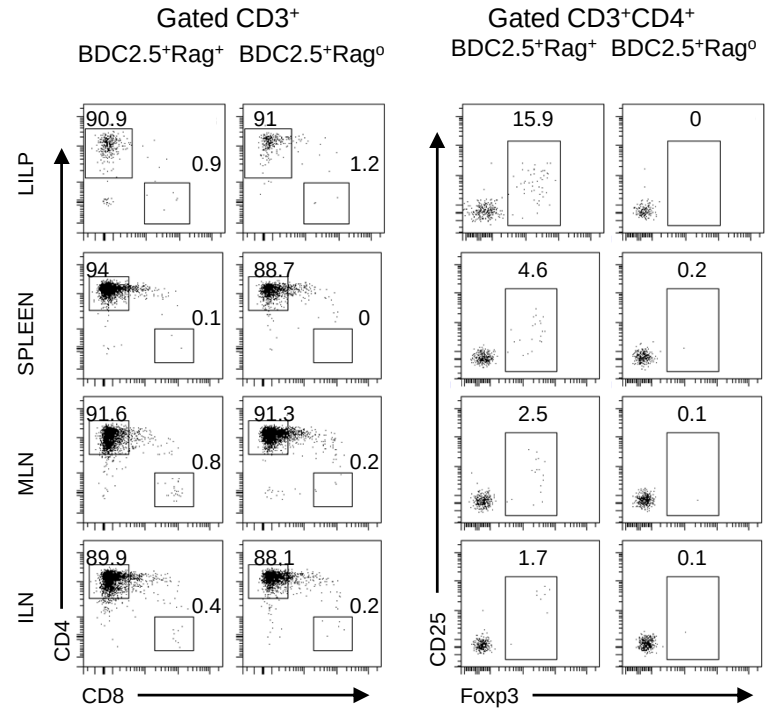
Gated CD3+
BDC2.5+Rag+
BDC2.5+Rago
Gated CD3+CD4+
BDC2.5+Rag+
BDC2.5+Rago
LILP
SPLEEN
MLN
ILN
90.9
0.9
91
1.2
94
0.1
88.7
0
91.6
0.8
91.3
0.2
89.9
0.4
88.1
0.2
15.9
0
4.6
0.2
2.5
0.1
1.7
0.1
CD4
CD8
CD25
Foxp3

Figure S3

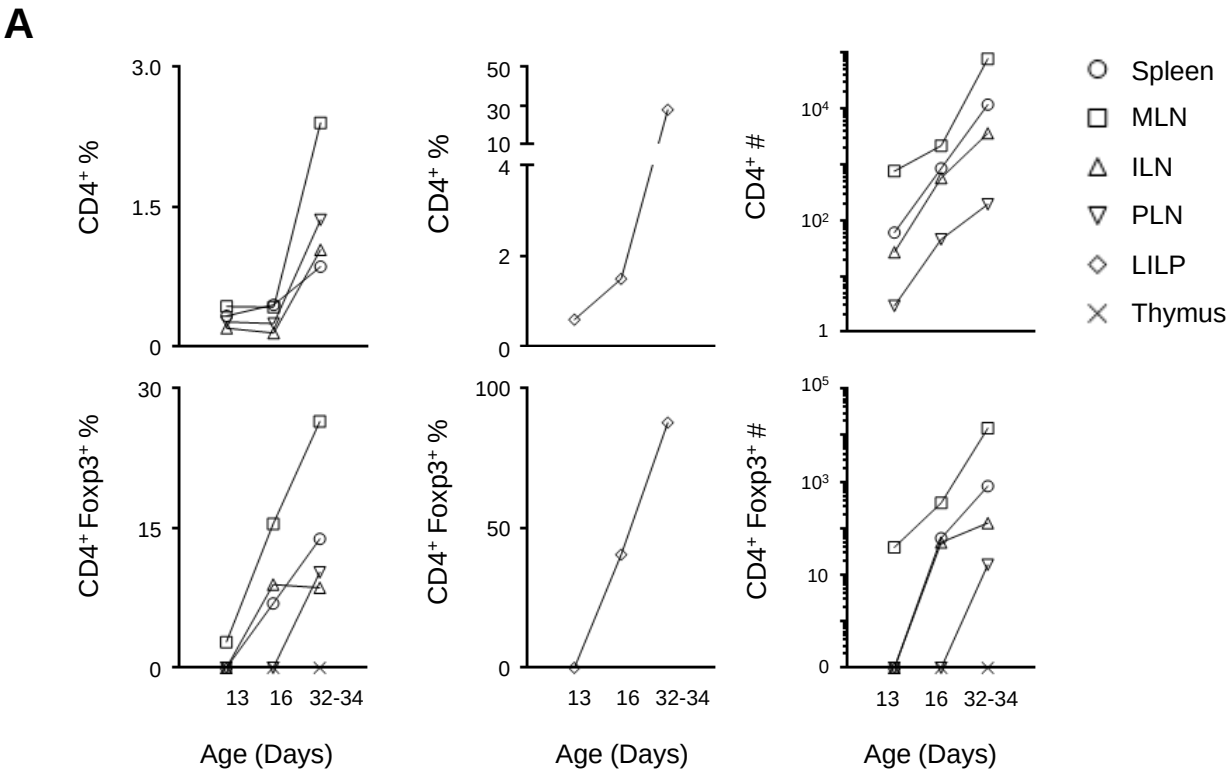
A
CD4+ %
CD4+ Foxp3+ %
CD4+ #
CD4+ Foxp3+ #
Spleen
MLN
ILN
PLN
LILP
Thymus
13
16
32-34
Age (Days)

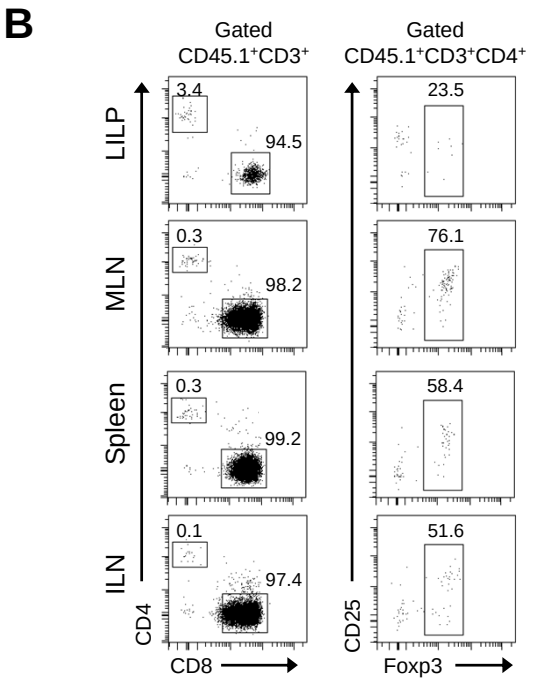
B
Gated CD45.1+CD3+
Gated CD45.1+CD3+CD4+
LILP
MLN
Spleen
ILN
3.4
94.5
0.3
98.2
0.3
99.2
0.1
97.4
23.5
76.1
58.4
51.6
CD4
CD8
CD25
Foxp3

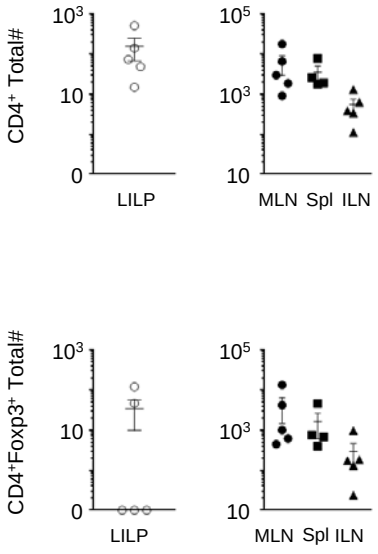
C
CD4+ Total#
CD4+Foxp3+ Total#
LILP
MLN
Spl
ILN

Figure S4

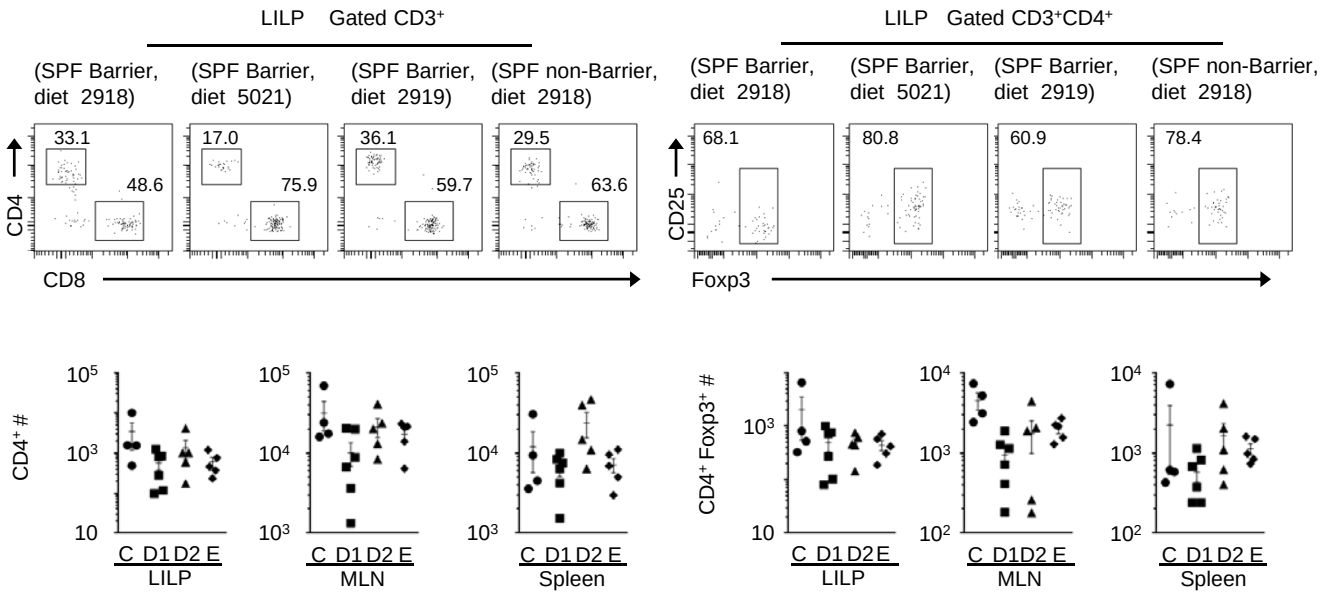

C: SPF Barrier, diet Teklad#2918 D1: SPF Barrier, diet LabDiet #5021

D2: SPF Barrier, diet Teklad #2919 E: SPF *non-Barrier*, diet #2918

Figure S5

A

Variable efficiencies of the CD8aCre transgene (xRosa26YFP$^+$) in marking CD8 lineage

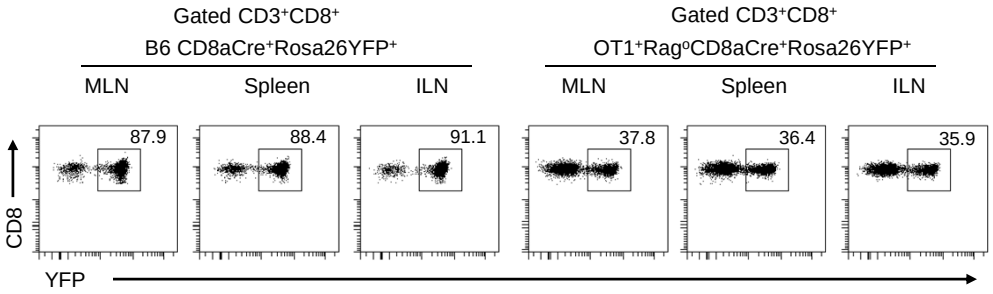

B

Analysis of B6 CD8aCre x Rosa26YFP mice at different age

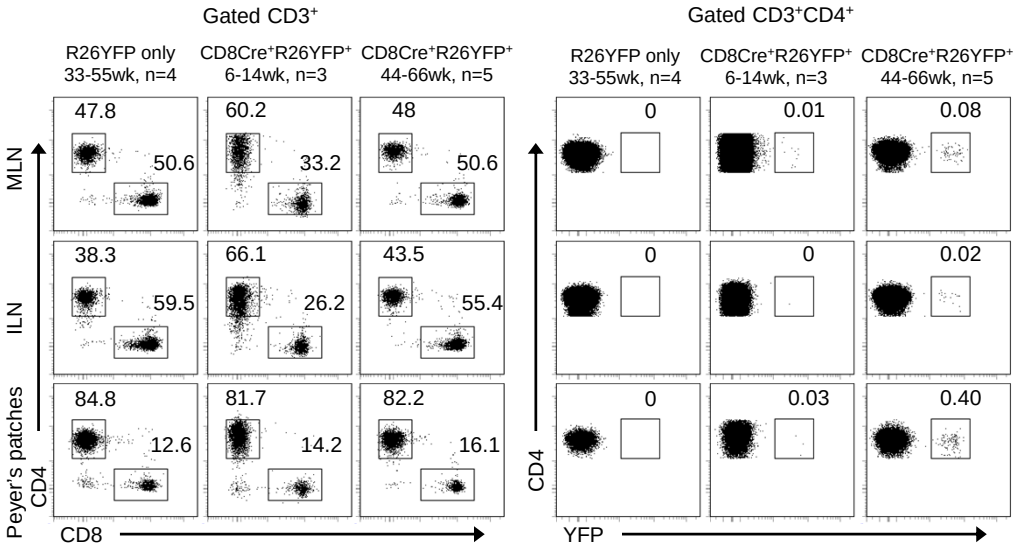

Figure S6

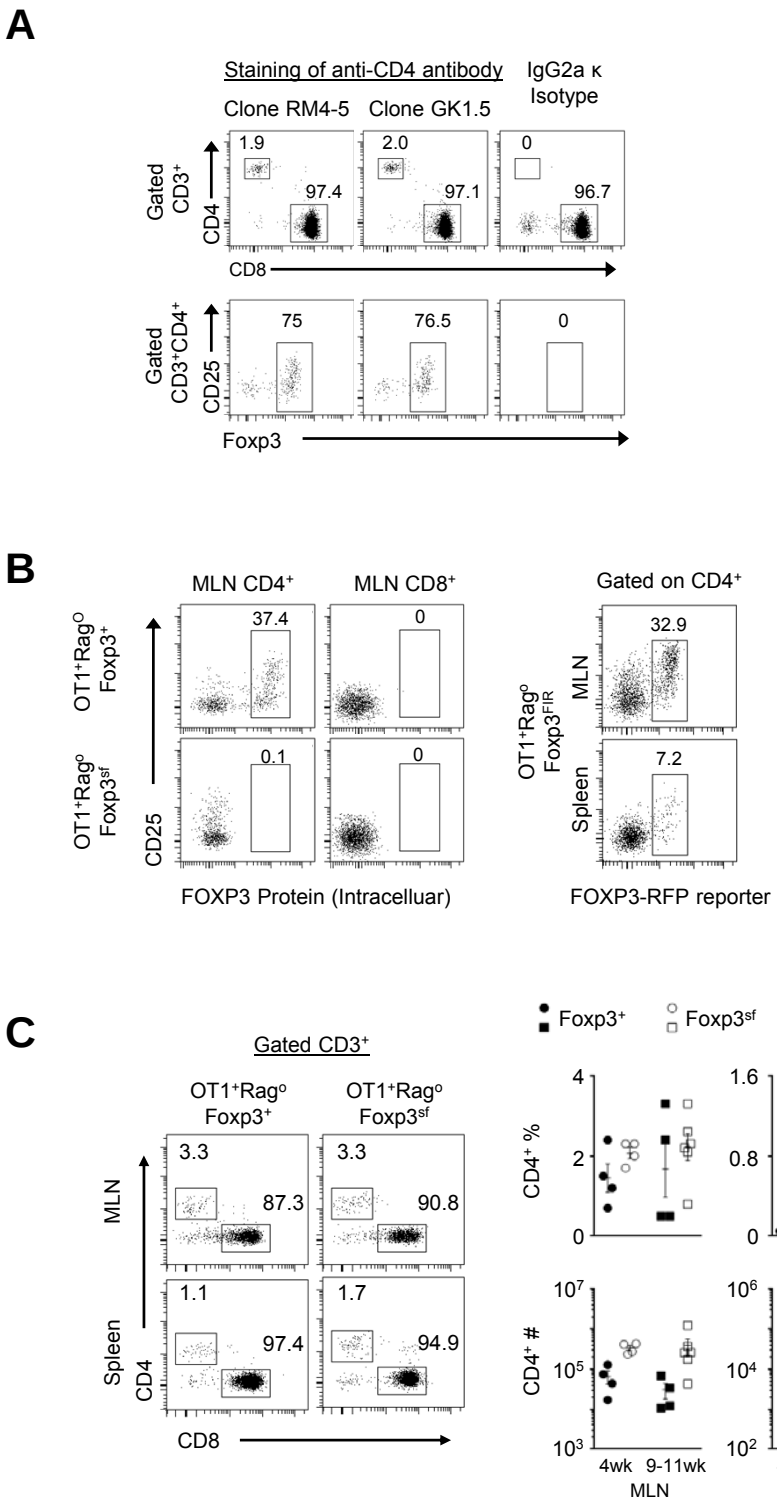
A
Staining of anti-CD4 antibody
Clone RM4-5
Clone GK1.5
IgG2a κ Isotype
Gated CD3+
CD4
CD8
1.9
97.4
2.0
97.1
0
96.7
Gated CD3+CD4+
CD25
Foxp3
75
76.5
0
B
MLN CD4+
MLN CD8+
OT1+Rag° Foxp3+
OT1+Rag° Foxp3sf
CD25
37.4
0
0.1
0
FOXP3 Protein (Intracelluar)
Gated on CD4+
OT1+Rag° Foxp3FIR
MLN
Spleen
32.9
7.2
FOXP3-RFP reporter
C
Gated CD3+
OT1+Rag° Foxp3+
OT1+Rag° Foxp3sf
MLN
Spleen
CD4
CD8
3.3
87.3
3.3
90.8
1.1
97.4
1.7
94.9
Foxp3+
Foxp3sf
CD4+ %
CD4+ #
*
**
4wk
9-11wk
MLN
Spleen

Figure S7

Supplemental Figure Legends

Figure S1 (relates to Figure 1).

Non-*MHC* genetic elements in the B6 genetic background, but not the autoimmune-prone NOD genetic background, promoted cross-differentiation from CD8 T-cell lineage to $CD4^+Foxp3^+$ CI-T_{reg} cells.

(A) Representative flow cytometry of LILP, MLN, Spleen, and PLN of NOD.8.3$^+$Rag^o and NOD/B6.8.3$^+$Rag^o mice compared at 6-8 wks of age (left), or NOD/B6.8.3$^+$Rag^o mice compared at 3 wks of age versus 6-8 wks of age (right).

(B) Summary of percentages and total cell counts of $CD4^+$ and $CD4^+Foxp3^+$ cells cross-differentiated from the 8.3 clone of the CD8 lineage in 6-8-wk-old NOD.8.3$^+$Rag^o mice (n=5, **black symbol**), 3-wk-old NOD/B6.8.3$^+$Rag^o (n=6, **gray symbol**) and 6-8-wk-old NOD/B6.8.3$^+$Rag^o mice (n=6, **open symbol**).

(**C**) Homozygosity of the *MHC* $H2^{g7/g7}$ on the mixed NOD/B6 genetic background did not preclude cross-differentiation of the 8.3 clone from the CD8 T lineage to the $CD4^+Foxp3^+$ T_{reg} cells, indicating the effect of genetic elements not linked to the *MHC* locus. NOD.8.3$^+$Rag^o mice were crossed with B6.Rag^o mice to produce 8.3$^+$Rag^o/NODxB6F1, which were backcrossed to the NOD genetic background (using NOD.Rag^o) for one generation (BC1). The BC1 offspring on the mixed B6/NOD genetic background were genotyped for heterozygosity or homozygosity of MHC haplotype $H2^{g7}$. The animals were then analyzed for presence or absence of $CD4^+Foxp3^+$ T cells by flow cytometry in the MLN. Out of the total 8 mice on the NOD/B6 BC1 mixed genetic background that had homozygous *MHC* $H2^{g7/g7}$, 4 mice had $CD4^+Foxp3^+$ (bottom panels) and the other 4 mice did not (middle panels).

*, $p<0.05$; **, $p<0.01$; ***, $p<0.001$.

Figure S2 (relates to Figure 1).

Cross-differentiated CD4 T cells from the CD8 lineage retained the TCR clonotype and responsiveness to MHC-class-I-restricted epitope and were predominantly Th1-like.

(A) OT1 TCR clonotype of $CD4^+$ and $CD4^+Foxp3^+$ T cells in $OT1^+Rag^o$ mice (n = 4) by flow cytometry analyses using antibodies against TCR Vα2 and Vβ5. As a negative control for the clonotype analyses, Vα2 and Vβ5 staining was performed on polyclonal lymphocytes from wildtype B6 mice.

(B) Splenocytes from $OT1^+Rag^o$ mice were labeled with CFSE and stimulated with the chicken ovalbumin (257-264) (SIINFEKL) peptides. After 90 hours of stimulation with MHC-class-I-restricted epitope, the cells were analyzed by flow cytometry for CFSE dilution. Representative flow cytometry plots were followed by summary of percentage of CD4 and CD8 OT1 T cells with CFSE dilution in response to the SIINFEKL peptide, compared to that without peptide stimulation. The numbers in the plots are percentages of the gated population. Data represent one of two experiments. Each data point represents one mouse (n=4; mean±SEM).

(**C**) Antigen-driven responses of purified CD4 OT1 cells to SIINFEKL peptides *in vivo.* B6 (CD45.2) mice were injected with 4-8 x 10^3 $CD4^+Foxp3^-$ cells purified from $OT1^+Rag^o$ CD45.1 congenic mice, and then immunized with the SIINFEKL peptides with lipopolysaccharide adjuvants, or PBS control with lipopolysaccharide adjuvants (n=3). Flow cytometry analyses were conducted 3 days later, using the CD45.1 congenic marker for identification of the adoptively transferred CD4 OT1 cells. Of note, no $CD45.1^+$ cells could be found in the mice that did not receive the specific peptide (the -SIINFEKL group in the left) but received the same number of CD4 OT1 cells, likely because the very low number (4-8 x 10^3) of the cells injected in the B6 mice. **(D-E)** The spleen and MLN of $OT1^+Rag^o$ mice were stimulated with phorbol dibutyrate (PDBU) and ionomycin for 6hrs and analyzed with intracellular staining for cytokine production. Left, representative flow cytometry; right; total numbers of cytokine-producing $CD3^+$ $CD4^+$ T cells. Of note, for both the MLN and the spleen, the low numbers of IL4- and IL17-producing cells contrast with the higher numbers of IFNγ-producing cells summarized in the plot. Each data point represents one animal (n=6; mean±SEM).

***, $p<0.001$.

Figure S3 (relates to Figure 2).

Absence of cross-differentiation from the CD4 lineage to CD8 cells in steady state of the large-intestine-associated microenvironment, illustrated with two independent clones in the MHC-class-II restricted CD4 lineage.

(A) Absence of large-intestine-associated cross-differentiation from the CD4 lineage to CD8 cells in the $OTII^{+}Rag^{o}$ model which consists of a monoclonal T-cell repertoire of the CD4 T-cell lineage**.** Flow cytometry of Rag-sufficient and Rag-deficient OTII TCR transgenic mice. Absence of CD4 to CD8 conversion was consistent in all $OTII^{+}Rag^{o}$ mice analyzed (n=4).

(B) Absence of large-intestine-associated cross-differentiation from the CD4 lineage to CD8 cells in the $BDC2.5^{+}Rag^{o}$ model which consists of a monoclonal T-cell repertoire of the CD4 T-cell lineage. Flow cytometry of Rag-sufficient and Rag-deficient BDC2.5 NOD mice. Of note, $BDC2.5^{+}Rag^{o}$ mice develop diabetes around 4 wks of age with a quick onset and progression due to a lack of regulatory T cells. Therefore, the analyses were conducted with non-diabetic animals at 20-24 days of age. The absence of CD4 to CD8 conversion was consistent in all $BDC2.5^{+}Rag^{o/o}$ analyzed (n=4).

Figure S4 (relates to Figure 3).

Kinetic evidence for the involvement of the large-intestine-associated microenvironment in the cross-differentiation from the CD8 lineage to CD4 T cells.

(A) Kinetics of cross-differentiation from the CD8 lineage to CD4 T cells in different organs of the $OT1^{+}Rag^{o}$ mice, with high frequencies in the large-intestine-associated microenvironment at an early age. Mean percentages and total cell numbers are shown for $CD4^{+}$ and $CD4^{+}Foxp3^{+}$ cells detected in the thymus, spleen, MLN, ILN, PLN and LILP in cohorts of $OT1^{+}Rag^{o}$ mice at 13 (n=3), 16 (n=4) and 32-34 (n=5) days of age.

(B-C) Cross-differentiation from the CD8 lineage to CD4 T cells occurred in $OT1^{+}Rag^{o}$ mice even after neonatal reconstitution with a large number of immune cells with a polyclonal repertoire. $CD45.1^{+}OT1^{+}Rag^{o}Foxp3^{FIR}$ B6 mice were injected with 20 million splenocytes from wildtype C57BL/6 donors (CD45.2, without the $Foxp3^{FIR}$ knockin allele) at 1 to 3 days after birth. The reconstituted mice were analyzed at 12-40 weeks of ages (n=5), for cross-differentiation of the host (CD45.1) OT1 clone from the CD8 lineage to CD4 T cells. Representative flow cytometry (**B**) was followed by $CD4^{+}$ and $CD4^{+}Foxp3^{FIR+}$ cell counts of the $CD45.1^{+}$ OT1 origin (**C**). Each data point represents one animal (n=5, mean±SEM).

Figure S5 (relates to Figure 4).

CD8-to-CD4 cross-differentiation in various settings of animal housing and diets.

To examine the effect of diet and environment, $OT1^{+}Rag^{o}$ mice were reared with different diets in SPF buildings (barrier or non-barrier). At 4-5 wks of age, $OT1^{+}Rag^{o}$ mice were analyzed for cross-differentiation from the CD8 T-cell lineage to CD4 T cells ($CD4^{+}$ or $CD4^{+}Foxp3^{+}$ populations). Top panels showing flow cytometry analyses of LILP samples with percentages of gated populations indicated in the plots. Bottom panels show cell counts of total CD4 and $CD4^{+}Foxp3^{+}$ cells in different organs. Each data point represents one animal (n=4-5, mean±SEM).

Figure S6 (relates to Figure 5).

Lineage tracing with CD8aCre x Rosa26YFP marking of peripheral CD8 T cells.

(A) Variable efficiencies of CD8 lineage marking by the CD8aCre transgenic model. The commercially available CD8aCre transgenic model, when crossed with the Rosa26YFP line for marking the CD8 lineage in the periphery, marked some but not the majority of CD8 T cells in the periphery of $OT1^{+}Rag^{o}$ mice. The transgenic line of Cre driven by an artificial CD8 promoter (Maekawa et al., 2008) was crossed with the Rosa26YFP mice and further crossed with $OT1^{+}Rag^{o}$ mice. The efficiency of CD8aCre x Rosa26YFP marking of CD8 T cells in the periphery was assessed by flow cytometry of $CD8aCre^{+}Rosa26YFP^{+}$ B6 mice (left) and $OT1^{+}Rag^{o}CD8aCre^{+}Rosa26YFP^{+}$ mice (right) (n=3-6), which carried the CD8aCre transgene and the Rosa26YFP knockin allele.

(B) Cross-differentiation from the CD8 lineage to CD4 T cells in non-TCR transgenic setting without involving adoptive transfer of T cells. Cross-differentiation of $CD8aCre^{+}Rosa26YFP^{+}$ T cells into CD4 T cells occurred rarely in un-perturbed mice. Flow cytometry analyses of the spleen, mesenteric lymph nodes, and Peyer's patches from $CD8aCre^{+}Rosa26YFP^{+}$ B6 mice at 6 wks and 44-66 wks of age.

Figure S7 (relates to Figure 6).

Foxp3 expression in the OT1^{+}Rag^{o} mice is restricted to the cross-differentiated CD4 T cells.

(A) CD4 expression in T cells from OT1^{+}Rag^{o} mice was examined with two different monoclonal antibodies specific to CD4 (clones RM4-5 or GK1.5) versus IgG2a κ isotype (n=3).

(B) Foxp3 expression in the CD4 T-cell population, but not CD8 T cells, in OT1^{+}Rag^{o} mice. The analyses were done by using both intracellular staining of Foxp3 proteins or Foxp3^{FIR} (Foxp3-IRES-Red Fluorescent Protein) "knockin" fluorescence reporter. The specificity of Foxp3-intracellular flow cytometry staining with monoclonal anti-Foxp3 antibodies was verified by staining MLN samples from Foxp3-deficient mice (Foxp3^{sf} null mutants). The numbers in the plot represent percentages of gated populations. Of note, most of the experiments in this study were conducted with aid of the Foxp3^{FIR} reporter line, but in some experiments intracellular staining with anti-Foxp3 antibodies was used to detect Foxp3 proteins.

(C) Conversion from the CD8 lineage to CD4 T cells did not require a functional Foxp3 gene. Left, representative flow cytometry plot for CD4 versus CD8 profile in OT1^{+}Rag^{o}Foxp3^{sf} mice versus OT1^{+}Rag^{o}Foxp3^{+} controls. Right, summary of CD4 cell counts in the MLN and spleen of the two group of mice at age of 4 weeks or 9-11 weeks (n=4-5, mean±SEM). **Closed symbols**, OT1^{+}Rag^{o}Foxp3^{+} mice; **Open symbols**, OT1^{+}Rag^{o}Foxp3^{sf} mice. The numbers in the flow cytometry plots represent percentages of gated populations. Each data point represents one animal. The increased CD4 cell counts in OT1^{+}Rag^{o}Foxp3^{sf} mice versus OT1^{+}Rag^{o}Foxp3^{+} controls were likely due to expansion in the absence of CD4^{+}Foxp3^{+} CI-T$_{reg}$ cells, similar to the expansion that occurred in the CD8 T cells (Figure 6).

*, $p<0.05$; **, $p<0.01$.

SUPPLEMENTAL EXPERIMENTAL PROCEDURES

Mouse diet and environment

The standard animal feed was Teklad Global 18% Protein Rodent Diet (Cat#2018, Harlan Laboratories, Madison, WI). To test the effects of diet, mice were reared on LabDiet Autoclavable Mouse Breeder Diet (#5021, LabDiet, St. Louis, MO) or Teklad Global 19% Protein Extruded Rodent Diet (#2019, Harlan Laboratories, Madison, WI). Neither Teklad Diets #2018 nor #2019 contains animal by-products. LabDiet #5021 contains ground fish by-products and porcine fat. Teklad Diet #2019 and LabDiet #5021 contain higher percentages of protein and fat content than Teklad Diet #2018.

Surgical removal of mesenteric lymph nodes

Thirteen- to 14-day old $OT1^{+}Rag^{o}$ mice were anesthetized. The abdomen was shaved and disinfected and an incision was made. The intestines and mesenteric lymph nodes (MLN) of the pups were exteriorized. The MLN were surgically excised. The mock surgery group underwent the same procedure except the exteriorized MLN was not excised. Intestines were reintroduced and the peritoneum was closed by suturing (Griffin et al., 2011). A dab of antibiotic ointment was placed along the peritoneum wounds and the skin was sutured closed with gut chromic suture line and sealed with surgical adhesive. The animals were sacrificed two weeks later, verified for lack of MLN (**Figure 3A**) and analyzed for immune cell phenotypes. At this end point, we did not detect visible sign of inflammatory damage in the peritoneal cavity in either the MLN removal group or the mock surgery group. Of note, both groups underwent the same major surgical procedures including incisions at the exterior and interior abdominal walls, exteriorization of the intestine and MLN, and suturing of the wounds on the two layers of peritoneal cavity wall, and therefore both groups were subjected to the inflammatory healing processes ensued from those major surgical procedures.

Thymectomy

Thirty- to 32- day old $CD8Cre^{+}Rosa26YFP^{+}$ B6 mice were anesthetized and their upper chest region was shaved and disinfected. A longitudinal incision was made along the skin above the sternum. A small incision was made at the sternal notch and forceps were used to hold open the incision. The thymus was vacuum

removed carefully with a cannula applying vacuum pressure. After removal, surgical adhesive was used to seal the wound and the skin was closed with surgical staples.

Antibody depletion of CD4 T cells

For CD4 T cell depletion, mice were injected i.p. two doses of 12 μg per gram of mouse body weight of anti-CD4 antibody (GK1.5) or Rat IgG controls five days apart. The efficacy of anti-CD4 antibodies in depleting CD4 T cells was verified by tail vein blood sampling after completion of treatment. The mice were then monitored for CD4 cell population recovery. The end point experiments were conducted 35-40 weeks after completion of anti-CD4 depletion.

Cell preparation from intestinal tissue and lymphoid organs

Single cell solutions of lymphoid organs were prepared according to standard procedure (Devarajan et al., 2014; Miska et al., 2014; Miska et al., 2012). For Peyer's patches, a thin rod was inserted into the small intestines and raised Peyer's patches were gripped with tweezers and dissected. Intestines were washed free of feces and minced in 2% fetal bovine serum (FBS) with PBS. Intestinal pieces were spun down, put in a solution of 2% fetal bovine serum, 1x HBSS, EDTA, and HEPES, and incubated at 37^{o}C for 15 minutes on a horizontal shaker set at 250 rpm. The supernatant was collected, washed with 2% FBS with PBS, and spun down to collect IELs. After extracting twice for IELs, the intestinal pieces were washed twice with 2% FBS with PBS to thoroughly remove residual EDTA. For lamina propria lymphocytes, intestinal pieces were placed in complete RPMI media with type IV collagenase (100U/mL)(Sigma, St. Louis, MO) and incubated at 37^{o}C for 1hr on a horizontal shaker set at 250 rpm. The dissociated tissue was filtered through an 80 micron filter and the cells were collected and washed by centrifugation.

Flow cytometry, cell sorting and adoptive transfer experiments

Flow cytometry analyses were conducted with a standard procedure (Devarajan et al., 2014; Miska et al., 2014; Miska et al., 2012). Cells were blocked from non-specific binding using a cocktail of anti-CD16/32 (2.4G2) and normal mouse sera (Jackson ImmunoResearch, Suffolk, UK). The cells were then stained with

fluorescent-antibody conjugates to determine cell phenotype. The following antibody conjugates were used: PE-Cy7 conjugated: anti-CD8, anti-CD11b, anti-CD11c, anti-Ter119, anti-B220, anti-NK1.1; APC conjugated: anti-CD4 and anti-Foxp3; PerCP-Cy5.5 conjugated: anti-CD25; APC-eFluor 780 conjugated: anti-CD62L; Alexa Fluor 700 conjugated: anti-CD3ε and anti-CD45.1; Alexa Fluor 488 conjugated: anti-CD8α, anti-TCRβ, anti-CD45.1, anti-Vα2 and anti-Foxp3; eFluor450 conjugated anti-CD44; PE conjugated: anti-TCRβ, anti-CD45.2, anti-Vβ5 and anti-Foxp3 (eBiosciences, San Diego, CA); Pacific Blue conjugated: anti-CD8α (Biolegend, San Diego, CA). For experiments in which T_{reg} cells were analyzed, $Foxp3^{FIR}$ reporter was used to identify Foxp3-producing cells. In some experiments, staining for intracellular Foxp3 protein with specific antibodies was used to verify Foxp3 expression. Stained samples were analyzed with LSR-II and Fortessa flow cytometers (Becton Dickinson, San Jose, CA).

In adoptive transfer experiments, CD8 T cells were sorted as $CD8^+CD4^-CD11b^-CD11c^-Ter119^-B220^-NK1.1^-CD25^-Foxp3^-$ from the spleen and lymph nodes of $OT1^+Rag^oFoxp3^{FIR+}$ mice or as $CD8^+YFP^+CD4^-CD11b^-CD11c^-Ter119^-B220^-NK1.1^-CD25^-Foxp3^-$ from $CD8Cre^+$ $Rosa26YFP^+$ mice. The purified CD8 T cells (purity > 99.7%), with or without the YFP marker, were injected into recipients. For neonate reconstitution of $OT1^+Rag^oFoxp3^{FIR+}$ mice, whole splenocyte preparation from B6 mice were injected, 2×10^7 cells per recipient, by intraperitoneal injection. To test antigen-driven responses of purified CD4 OT1 cells to SIINFEKL peptides *in vivo*, 4-8 x 10^3 $CD4^+Foxp3^-$ cells purified from $OT1^+Rag^o$ CD45.1 congenic mice were injected into B6 (CD45.2) mice. Twelve hours later, the animals were immunized with 10 μg SIINFEKL peptides with lipopolysaccharide adjuvants, or PBS control with lipopolysaccharide adjuvants. The animals were analyzed 3 days post immunization.

Intracellular cytokine analysis

For IFNγ and IL17 cytokine analysis, cells from the spleen and MLN of $OT1^+Rag^oFoxp3^{FIR}$ mice were cultured in complete RPMI media with 40nM phorbol dibutyrate (PDBU) and 2uM ionomycin for 1 hour at 37°C (4×10^6 cells per mL). After 1 hour, Brefeldin A was added and incubated for another 5 hours. For IL4 cytokine analyses, cells were stimulated as above for 4 hours before Brefeldin A was added and incubated for additional 2 hours. Intracellular cytokines were stained by flow cytometry following a standard procedure.

CFSE assay for cell proliferation

The spleen and lymph node cells were prepared to single cell solution and labeled with carboxyfluorescein diacetate, succinimidyl ester (CFSE) (Life Technologies, Grand Island, NY) according to a standard procedure. The labeled cells were stimulated *in vitro* with the standard ovalbumin peptide (SIINFEKL) that elicited MHC-class-I restricted responses in the OT1 T cell clone. After 90hr of stimulation, the cells were stained with CD3, CD4 and CD8 and analyzed for CFSE dilution of the specific T-cell subsets.

Colitis studies

Two-month old $OT1^{+}Rag^{o}Foxp3^{+}$ and $OT1^{+}Rag^{o}Foxp3^{sf}$ mice were administered 4% dextran sodium sulfate (DSS) (MP Biomedicals, Santa Ana, CA) in drinking water for 6 days. Mice were then switched to normal drinking water and monitored for one week. The animals were monitored daily for weight as well as signs of diarrhea. During the monitoring period, mice showing two consecutive days of weight loss for more than 20% of the original weight and apparently moribund were sacrificed, as required by institutional standard protocols. Otherwise, all animals were sacrificed the day after the pre-set monitoring period. Intestinal tissue samples were fixed in formalin solution. Paraffin embedded sections were stained with hematoxylin and eosin (H-E) and examined by microscopy.

We also used a model of colitis induced with naïve CD8 T cells (Tajima et al., 2008). In the original study, 5×10^5 CD8 T cells were injected into each Rag^{o} recipients (Tajima et al., 2008). For co-transfer of CI-T_{reg} cells in our studies, although the OT1 $CD4^{+}Foxp3^{+}$ CI-T_{reg} cells were relatively abundant in the LILP of $OT1^{+}Rag^{o}$ mice, the enzymatic digestion of tissue and isolation of cells largely reduced the viability of the cells. Therefore, we used the MLN and spleen for the purification of CI-T_{reg} cells, which had only a low frequency in the lymphoid organs. We pooled several $OT1^{+}Rag^{o}$ mice to purify ~7×10^4 OT1 $CD4^{+}Foxp3^{+}$ cells in each experiment. To facilitate a likely effective ratio (1:3) with the CD8 T_{eff} cells, we used 2×10^5 CD8 cells for each Rag^{o} recipient. The mice were monitored for potential weight loss. The colitis pathology was scored in a range of 0-3 according to the criteria described before (Tajima et al., 2008).